Numerical modelling of the seismic response of a half-scale stone masonry aggregate prototype

Ilaria Senaldi [a,b], Gabriele Guerrini[a,b], Marco Solenghi[a], Francesco Graziotti[a,b], Andrea Penna[a,b], Katrin Beyer[c],
[a] *Department of Civil Engineering and Architecture (DICAr), University of Pavia, Via Ferrata 3, 27100 Pavia, Italy*
[b] *European Centre for Training and Research in Earthquake Engineering (EUCENTRE), Via Ferrata 1, 27100 Pavia, Italy*
[c] *École Polytechnique Fédérale de Lausanne (EPFL), Bâtiment CE 3316, Station 1, CH - 1015 Lausanne, Switzerland*

Keywords: Stone masonry, equivalent frame, nonlinear macroelement, flexible diaphragm, nonlinear dynamic analysis

ABSTRACT
Basel is one of the most vulnerable regions within Switzerland. Hence, the local and regional authorities promoted an extensive experimental and numerical research project to assess the seismic vulnerability of existing stone masonry buildings, in order to identify suitable strengthening strategies to preserve the cultural heritage. A shaking table test was therefore performed on a three-storey half-scale prototype of a natural stone masonry building aggregate with flexible timber diaphragms, incorporating the main architectural and structural features of existing buildings in Basel's historical center. The test was performed up to near-collapse conditions of the specimen, using input ground motions representative of realistic seismic scenarios for the examined region.
The experimental response of the prototype was simulated by means of nonlinear static and nonlinear dynamic analyses. The structure was modeled following an equivalent frame approach with nonlinear macroelements, in order to replicate both the global behaviour of the structure and the local out-of-plane overturning response. An unconventional modelling strategy was adopted to implement explicitly the out-of-plane stiffness of the walls orthogonal to the shaking direction, through a combination of equivalent frames and membranes.
Numerical and experimental results were compared in terms of pushover and backbone curves, hysteretic responses, and lateral displacement envelopes. The consistency between numerical simulations and experimental results was also verified in terms of damage pattern and activation of failure mechanisms.

1 INTRODUCTION

The results presented in this work are part of a wider research project, jointly carried by the University of Pavia and the École Polytechnique Fédérale de Lausanne, which aims at assessing the seismic response of natural stone masonry buildings typical of the city of Basel, Switzerland.

As part of a comprehensive experimental campaign, a unidirectional, incremental dynamic shake-table test on a three-storey half-scale unreinforced masonry building aggregate was performed at the EUCENTRE laboratory in Pavia, Italy (Senaldi et al., 2019; Guerrini et al., 2019). The prototype reproduced typical features of existing buildings in Basel's historical centre.

The building aggregate prototype was modelled following an equivalent frame approach with nonlinear macroelements. The structural response at each stage of testing was simulated performing nonlinear static and nonlinear dynamic analyses. The purpose of this numerical investigation was to address the contribution of the out-of-plane stiffness of masonry walls to the overall structural behaviour, adopting unconventional modelling strategies.

2 OVERVIEW OF THE PROTOTYPE

The prototype building aggregate consisted of two adjacent weakly connected three-storey structural units, characterized by different roof heights and sharing the central transverse wall to emulate typical continuous building aggregates along the streets. The specimen reproduced the architectural and structural features of existing buildings typical of the historical centre of Basel.

The prototype was constructed in half-scale due to the limited dimensions of the shaking table. The entire aggregate was 5.79-m long and 5.58-m wide (Figure 1), and was constructed directly on composite concrete-steel foundations fixed to the

shaking table (7.00-m long, 5.60-m wide). The longitudinal West and East walls were oriented parallel to the shaking direction (Figure 2). The roof ridges of the two units were approximately 6.65-m and 7.60-m high. Furthermore, three façades showed aligned openings, with the exception of the South wall.

The building aggregate prototype was characterized by timber floors and roofs. Flexible floor diaphragms consisted of timber joists (with typical section of 10x16 cm) and of 2-cm thick planks, nailed to the joists (Figure 3). The first- and second-floor joists were oriented in the North-South direction, parallel to shaking, while the roof trusses were perpendicular to the longitudinal façades (Figure 3 and Figure 4).

The roof trusses were stiffened by diagonal and cross bracings (Figure 4), as typically found in Basel historical building, forming three-dimensional timber structures, on which purlins and clay tiles were directly attached without planks.

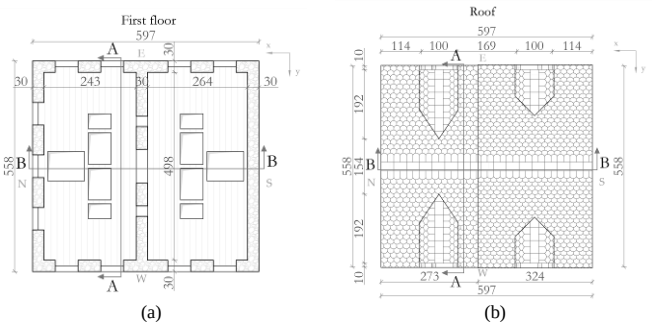

Figure 1. Plan views of the prototype: (a) first floor, (b) roof.

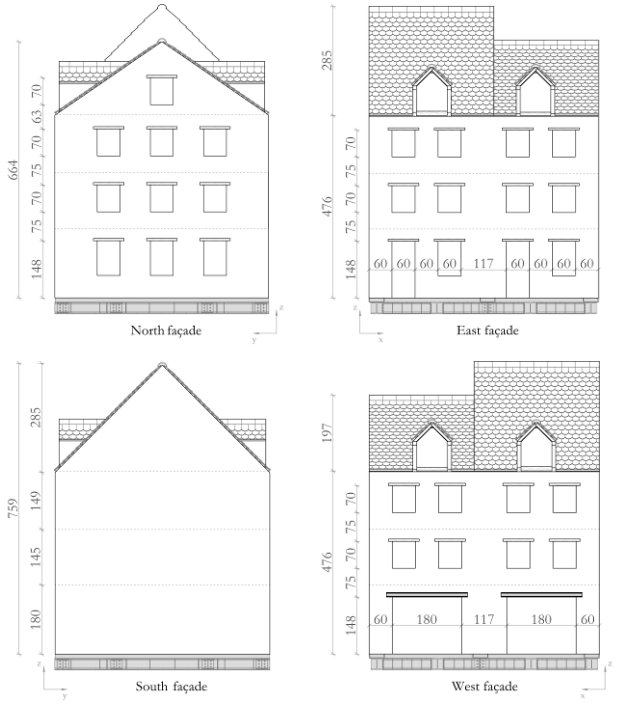

Figure 2. Elevation views of the façades.

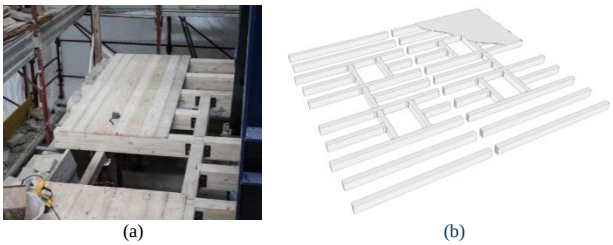

Figure 3. Second floor diaphragm: (a) orientation of beams and planks, (b) 3D rendering.

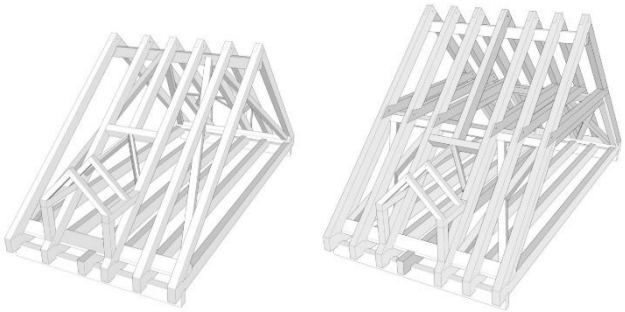

Figure 4. 3D renderings of roof trusses: (a) pitches with 35° slope, (b) pitches with 45° slope.

Figure 5. Masonry configuration: (a) front view, (b) horizontal section.

As previously mentioned, the roof structures are characterized by different slopes (34° and 45°, respectively) and consequently by two different truss configurations (Figure 4). The shallowest truss was a simple triangle, while the tallest one was more complex with a collar tie beam and a supporting secondary structure.

Walls were constructed with double-leaf undressed stone masonry (Figure 5), with 10% to 15% in volume of river pebbles of approximately 5-cm diameter, to reproduce the historical construction materials of the city. Stones were arranged in almost horizontal courses, though not perfectly regular given the variable dimensions of blocks and pebbles. Through stones were located only in correspondence of openings and corners, although not in every masonry course, providing a better connection between masonry leaves.

The perimeter wall thickness decreased along the height of the building, from 35 cm at the first storey, to 30 cm at the second storey, and to 25 cm at the third storey and in the gables. Furthermore, the wall thickness was reduced to 15 cm in correspondence of spandrels, constructed with a single masonry leaf above the floor level.

Table 1. Summary results of mechanical characterization tests on masonry wallettes.

	f_c [MPa]	f_t [MPa]	E [MPa]	υ [-]	G [MPa]
Mean	1.30	0.17	3462	0.14	1898
St.dev.	0.03	0.012	418	0.08	1104
C.o.v.	2.6%	7.3%	12%	56%	58%

Because of similitude requirements, strength and elastic modulus of the masonry were reduced by the same 0.5 geometrical scaling factor, with respect to the reference characteristics. The actual mechanical properties of the specimen materials were evaluated through characterization tests (Guerrini et al., 2017) and are summarized in Table 1, in terms of Young's modulus E, compressive strength f_c, Poisson's modulus υ, tensile strength f_t and shear modulus G (the latter obtained from diagonal compression tests).

3 SHAKE-TABLE TESTS

An incremental dynamic test was conducted on the building prototype, by gradually increasing the intensity of the input table motion.

Three different natural accelerograms were selected for the test (Table 2). The input "BAS" and "LIN" were recorded during recent seismic events occurred in Basel and in the Linthal valley, Switzerland. The accelerogram "MON" refers to the 1979 Montenegro earthquake, recorded at the Ulcinj Albatros Hotel station. The latter is spectrum-compatible in displacement with the 475-years-return-period elastic design spectrum for the city of Basel (Fäh and Wenk, 2009; Wenk and Fäh, 2012), within a period range characteristic of masonry structures (i.e., between 0.1 s and 0.6 s).

All records were scaled in time, because of similitude relationships, by a factor equal to the square root of the geometrical scaling factor (Senaldi et al., 2019). Table 3 summarizes the sequence of main shocks imposed to the building specimen, specifying the scale factor of the reference input signal.

Table 2. Summary of selected records.

Name	M_w	PGA [m/s^2]	I_{HM} [m]	CAV [m/s]	Duration [s]
Basel	3.4	0.707	0.006	0.3574	14
Linthal (2017)	4.7	0.852	0.016	0.3614	11
Montenegro (1979)	6.9	2.198	0.139	7.4263	41

Table 3. Testing sequence with recorded PGA values.

Input motion (Scale factor)	PGA [g]
BAS (100%)	0.052
LIN(100%)	0.053
MON (25%)	0.047
MON (50%)	0.098
MON (75%)	0.174
MON (100%)	0.204
MON (125%)	0.269
MON (150%)	0.321
MON (175%)	0.347

4 NUMERICAL SIMULATIONS

In order to simulate the experimental response of the specimen, nonlinear static analyses and incremental dynamic analyses were performed on a three-dimensional model of the building based on the equivalent frame approach implemented in TREMURI (Lagomarsino et al., 2013).

4.1 Modelling assumptions

Following the equivalent frame approach, each masonry wall is subdivided into an assembly of deformable panels (piers and spandrels), where deformations and nonlinear response are concentrated, and rigid nodes that connect the deformable panels.

The in-plane behaviour of each masonry panel was modelled using the nonlinear macroelement described by Penna et al. (2014) and further improved by Bracchi et al. (2018). This macroelement allows representing the two main in-plane masonry failure modes, bending-rocking and shear-sliding mechanism including friction, as well as their mutual interaction. The shear-sliding damage evolution, which controls strength deterioration and stiffness degradation, and toe-plasticization effects in the bending-rocking mode, are implemented through internal variables.

Masonry mechanical proprieties were calibrated simulating the nonlinear response exhibited by piers subjected to in-plane cyclic shear compression tests (Senaldi et al., 2018), through cyclic pushover analyses. Table 4 summarizes the mechanical properties assigned to the nonlinear macroelements. Parameters Gc_t and β define the peak displacement and the softening branch of the masonry inelastic constitutive relationship.

Table 4. Masonry mechanical properties adopted for the nonlinear macroelement.

f_c	f_t	E	G	Gc	β
[MPa]	[MPa]	[MPa]	[MPa]	[-]	[-]
3.58	0.187	2310	1024	10	0.5

The formulation of the in-plane equivalent frame model in TREMURI neglects the wall out-of-plane contribution to strength and stiffness. However, the experimental behaviour exhibited by the prototype during the shake-table tests was characterized not only by the in-plane response of the longitudinal façades, but also by out-of-plane overturning mechanisms of the transverse walls.

Hence, since these mechanisms may have significantly affected the global behaviour of the prototype, an unconventional modelling strategy was adopted, following the same approach proposed by Kallioras et al. (2019). The out-of-plane response of the transverse walls was explicitly modelled implementing two systems with different purposes.

The first system consisted of a set of equivalent frames (Figure 6.a and b) aiming at replicating the in-plane and out-of-plane stiffness components of transverse walls and gables. The in-plane contribution of transverse walls was accounted for by modelling piers acting as return walls and vertical elastic beam elements located in the transverse walls plane (Figure 6.a). These pier and beam elements were connected to the longitudinal walls by horizontal linear elastic beam elements with stiffness equivalent to that of the masonry walls portion considered to be effective. An equivalent frame defined in a plane parallel to the direction of shaking was then connected to the transverse walls at mid-span to model the out-of-plane stiffness of the transverse walls subjected to vertical bending (Figure 6.b).

The second system (Figure 7) consisted of linear elastic orthotropic membranes with three nodes, whose shear stiffness was taken equivalent to the out-of-plane stiffness of the transverse walls subjected to horizontal bending between each longitudinal wall and the equivalent frame of Figure 6.b, over a length L (Figure 7.c). The membranes equivalent shear modulus G_{eq} was defined by equating the elastic shear stiffness of the membrane to the flexural stiffness of the transverse wall vertical cross section assuming double-fixed boundary conditions:

$$\frac{G_{eq}A}{\chi L} = \frac{12E\left(\frac{\bar{h}t^3}{12}\right)}{L^3} \quad \Rightarrow \quad G_{eq} = 2 \cdot \chi \cdot \frac{E\bar{h}t^3}{sbL^2} \qquad (1)$$

In the previous equation, E is the masonry Young's modulus of the masonry, $\chi = 1.2$ is the shear factor, t and $\bar{h}$ are the thickness and the height of the panel's portion considered to be involved in the mechanism, L is the half-length of the transverse wall (Figure 7.c), b is the width of the floor mesh in which the membrane was defined (orthogonal to L), s is the membrane thickness, and $A = s \cdot b/2$ is the membrane average cross-section area.

Timber floors and roof diaphragms were discretized as two-dimensional orthotropic membranes with four nodes and linear elastic shear stiffness evaluated following the relationship proposed by Brignola et al. (2008).

4.2 Numerical analyses

The numerical investigations included both nonlinear static (pushover) analyses and nonlinear dynamic analyses.

Nonlinear static analyses were performed considering two different distribution of horizontal forces. The first one (named as "Pattern 1") consisted of a load distribution proportional to the nodal masses, while the second one ("Pattern 2") consisted of an inverse triangular load pattern.

Nonlinear dynamic analyses were conducted consecutively one for each test listed in Table 3, adopting as input the acceleration signals recorded by the accelerometer located on the shaking table. As previously mentioned, the effects of damage accumulation on piers and spandrels was explicitly accounted for.

Furthermore, Rayleigh viscous damping model was adopted, calibrating the parameters as suggested by Penna et al. (2016) to represent the variation of dissipative response as the dynamic properties varied due to increasing damage. Hence, the damping ratio was decreased from 5% for tests LIN100% through MON75%, to 3% for tests MON100% and MON125%, and finally to 2% for tests MON150% and MON175%.

The results of the numerical simulations were then compared with the damage pattern observed in the laboratory and to the dynamic response experimentally recorded by the instrumentation installed on the prototype.

4.3 Comparison between numerical and experimental results

The global capacity curves of the prototype, obtained from the pushover analyses, were compared with the backbone curves obtained from nonlinear dynamic analysis and from the shake-table experiment, as reported in Figure 8.

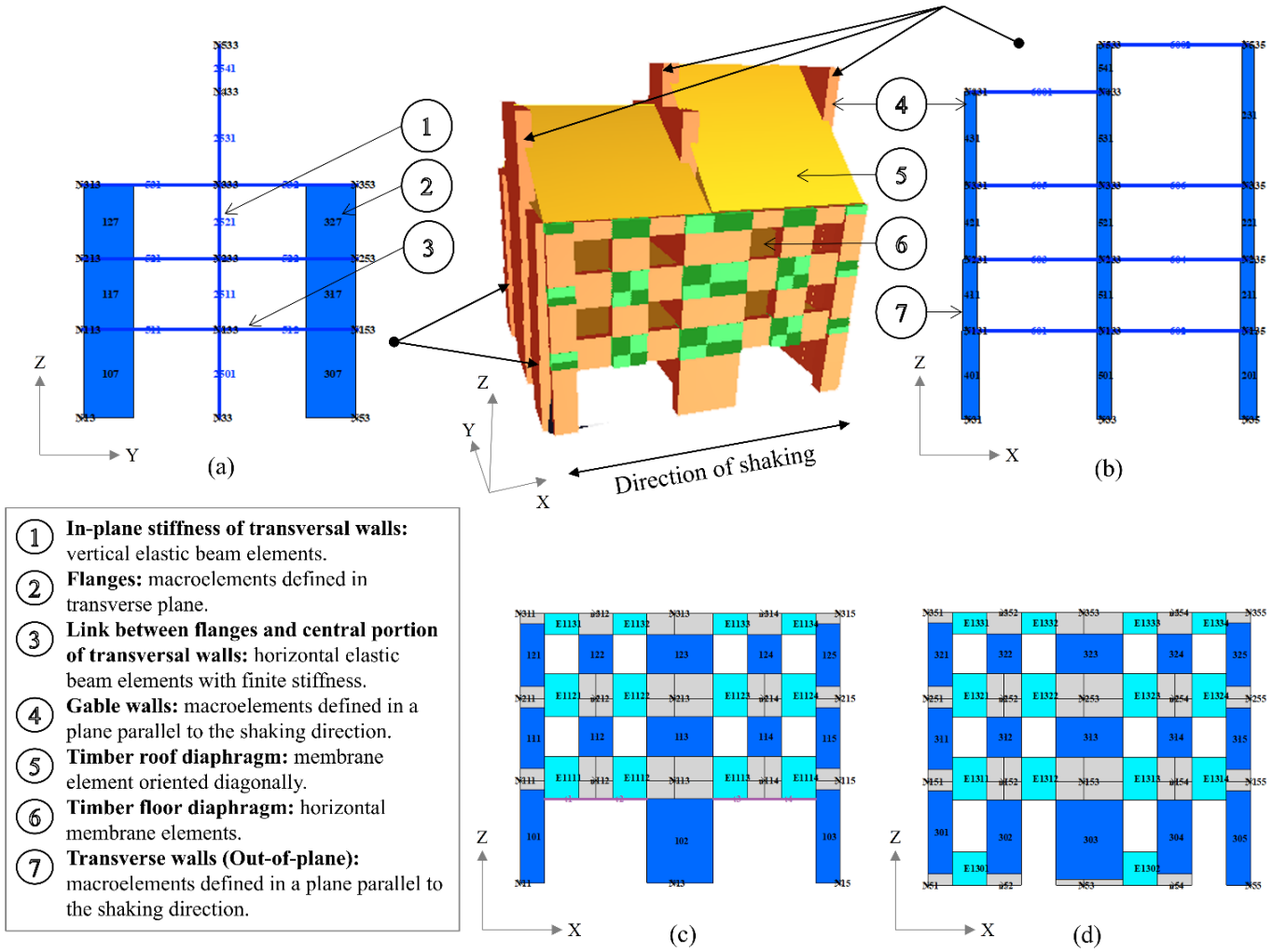

Figure 6. Different components of the numerical 3D model of the prototype: (a) pier and elastic beam elements capturing in-plane behaviour of a transverse wall, (b) equivalent frame parallel to the shaking direction capturing the out-of-plane contribution of the transverse walls in their vertical plane, (c) longitudinal West wall, (d) longitudinal East wall.

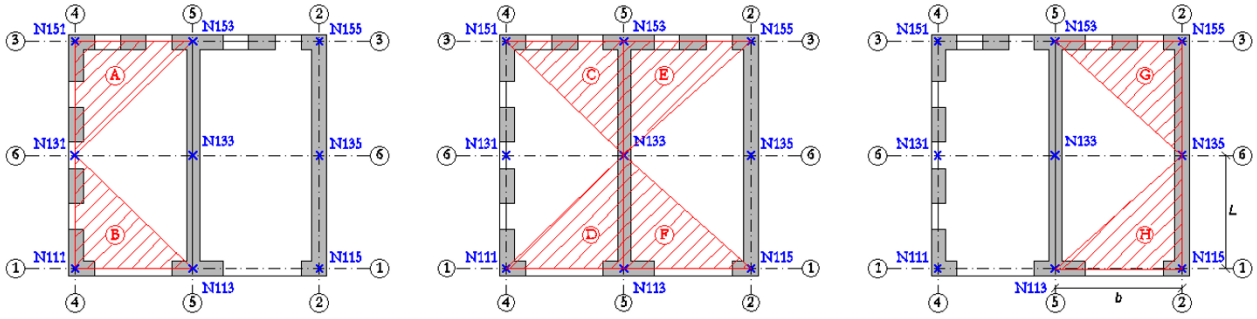

Figure 7. Three-nodes membranes capturing the out-of-plane stiffness component of the transverse walls in the horizontal plane: (a) North wall, (b) Central wall, (c) South wall.

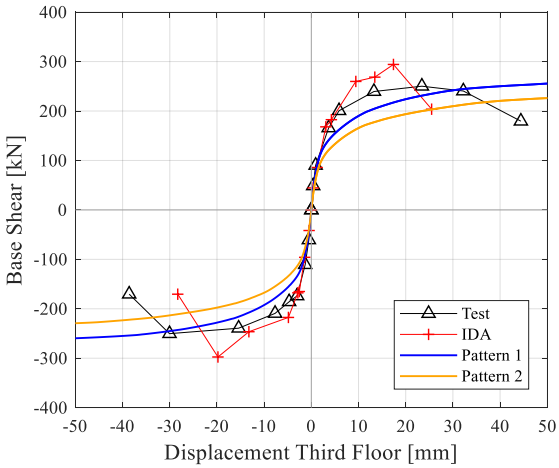

Figure 8. Global capacity curves of the prototype: experimental backbone (black), nonlinear dynamic analysis backbone (red), pushover analysis with load pattern 1 (blue), and pushover analysis with load pattern 2 (orange).

Backbone curves from the experimental response of the specimen (in black) and from dynamic analysis (in red), were obtained as the envelope of the hysteretic curves of each dynamic test, taking the points at maximum base shear with the associated average third-floor displacement. The base shear was determined as the sum of the inertia forces at each node location, as the product of its tributary mass times the corresponding acceleration, explicitly accounting for the contribute of the out-of-plane response of transverse walls. Pushover curves were reported for the mass-proportional load pattern (in blue) and for the inverse triangular load pattern (in orange).

Figure 8 shows that the incremental dynamic analysis provided quite accurate results in terms of global stiffness estimation, with fairly good displacement demand prediction until test MON100%. However, in higher-intensity tests (MON125%, MON150% and MON175%), overprediction of the global stiffness of the specimen can be noted, due to overestimation of the stiffness associated to the out-of-plane contribution of the transverse walls, with the maximum shear base about 22% larger than the experimental one. On the other hand, the pushover analysis with mass-proportional load pattern showed good accuracy in lateral strength estimation, despite the global stiffness was slightly underestimated.

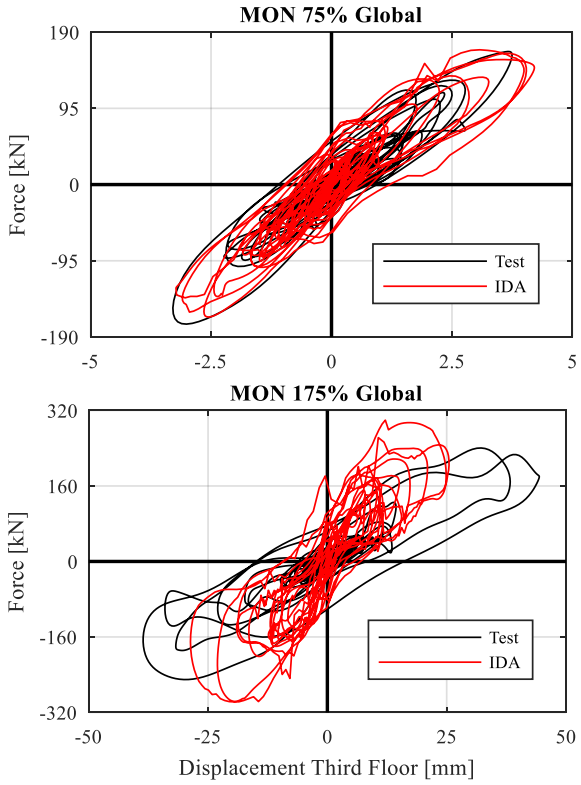

Figure 9. Global hysteretic response: experimental (black) and numerical (red) response. Tests with different seismic input: MON75% (top) and MON175% (bottom).

The accuracy of the incremental dynamic analysis in simulating the nonlinear behaviour of the prototype is evidenced by the comparison of the numerical and experimental global hysteretic curves showed in Figure 9 for the tests MON75% and MON175%,. The adopted modelling strategy (plotted in red) caught efficiently the hysteretic response exhibited by the building during the experimental test MON75% (in black), when the structure was still in the elastic range. However, as the response became increasingly nonlinear because of accumulation of damage, as in the test MON175%, the model overestimated the global stiffness and underestimated the ultimate displacement demand.

The damage patterns on longitudinal walls resulting at the end of the nonlinear dynamic analyses (test MON175%) were reported in Figure 10, together with details of the actual damage surveyed after the shake-table tests. The numerical damage level is identified by different colours and symbols: red identifies elements that reached the peak shear strength, while the cross indicates the full development of a shear mechanism. Straight lines represent flexural cracking.

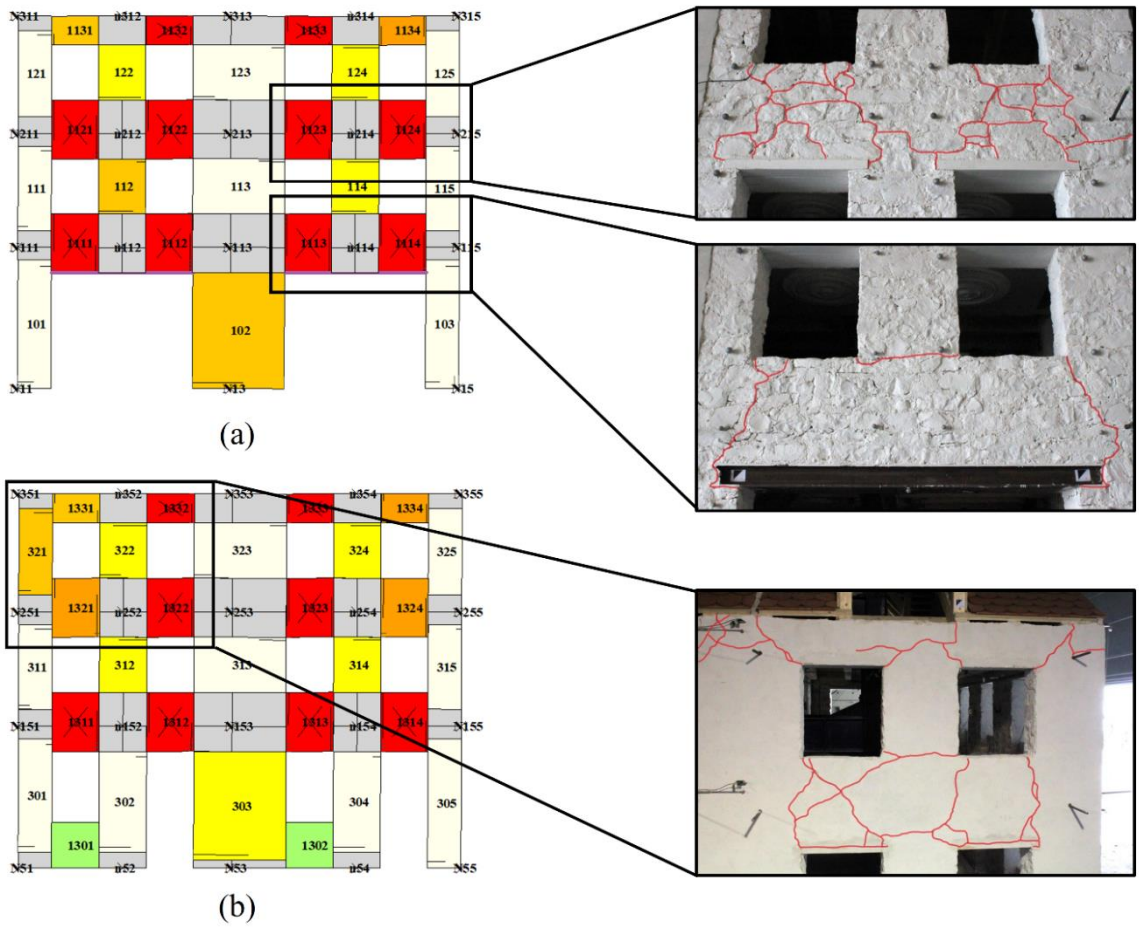

Figure 10. Numerical damage patterns on longitudinal walls evaluated with incremental dynamic analysis: (a) West wall at the end of Test MON175%, (b) East wall at the end of Test MON175%. Comparison with details of the experimentally observed damage (crack patterns highlighted in red).

Comparing the predicted damage on the longitudinal façades with the one observed experimentally, the adopted modelling strategy was able to reproduce with good approximation the mechanisms occurred in piers and spandrels (Figure 10), despite the limited accuracy in capturing the stiffness of the structure close to the ultimate limit state. In fact, the model correctly captured the flexural crack patterns at the base of ground-floor masonry piers, which exhibited a prevalently flexural behaviour, as well as the development of shear mechanisms as observed on most of the spandrels of both West and East façades.

The only major discrepancy between numerical and experimental damage patterns was found in the West-wall spandrel elements above the steel lintel of the large ground-floor openings. As shown in Figure 10.a, the macroelements corresponding to those spandrels fully developed shear mechanisms that were not observed on the prototype at the end of test MON175%.

The difference between pushover analyses results and experimental behaviour is also evident in terms of damage pattern at ultimate limit state. From the pushover analyses, a concentration of damage at the ground floor resulted in a soft-story mechanism which is in contrast with the experimental behaviour of the prototype, with largest discrepancy in the case of inverse triangular load pattern.

5 CONCLUSIONS

A shake-table test was conducted on a half-scale prototype of a stone masonry building aggregate with flexible timber diaphragms, representing two units with structural and architectural features representative of Basel, Switzerland, historical centre. The test was numerically simulated with a three-dimensional equivalent-frame model of walls responding in their plane, based on nonlinear masonry macroelements and linear diaphragm membranes in the software TREMURI. An unconventional

modelling strategy was adopted to include the effects of walls subjected to out-of-plane excitaiton, which required the introduction of auxiliary frame and membrane elements.

Nonlinear dynamic analyses proved to be an effective tool for the simulation of the experimental response of the half scale aggregate building prototype. The incremental dynamic analysis was able to reproduce the hysteretic behaviour of the structure as well as the distribution of accelerations and the effects due to the accumulation of damage in masonry structural elements. These aspects were not captured with the same accuracy by monotonic nonlinear static analyses.

Explicit modelling the out-of-plane stiffness of the prototype walls proved effective at capturing the stiffness and hysteretic behaviour of the prototype up to the attainment of a slight-to-moderate damage level. However, during the simulation of subsequent higher-intensity tests, the numerical response was characterized by an overestimation of the global stiffness, because of an overprediction of the out-of-plane contribution.

The unconventional modelling strategy applied to include the out-of-plane wall response will be the object of further developments. For example, a better simulation of the prototype dynamic response could be obtained by developing equivalent membrane elements with elasto-plastic behaviour, currently not implemented in TREMURI, capable to capture with better approximation the stiffness degradation associated with the progressive activation of out-of-plane overturning mechanisms.

ACKNOWLEDGEMENTS

The work presented is part of the research project “Seismic assessment of natural stone masonry buildings in Basel - A research and training project”, jointly carried by the École Polytechnique Fédérale de Lausanne and the University of Pavia, which was supported by the Swiss Federal Office for the Environment and the Construction Department of the Canton Basel-Stadt.

REFERENCES

Bracchi, S., Galasco, A., Penna, A., Magenes, G., 2018. An improved macroelement model for the nonlinear analysis of masonry buildings. *10th Australasian Masonry Conference*, February 11-14, Sydney, Australia.

Brignola, A., Podestà, S., Pampanin, S., 2008. In-plane stiffness of wooden floor. *2008 NZSEE Conference*, April 11-13, Wairakei, New Zealand.

Fäh, D., Wenk, T., 2009. *Mikrozonierung für die Kantone Basel Stadt und Basel Landschaft, Optimierung der Form der Antwortspektren und der Anzahl der Mikrozonen. Abschlussbericht: Teilbericht B*. Report, Swiss Seismological Service, ETH Zurich.

Guerrini, G., Senaldi, I., Scherini, S., Morganti, S., Magenes, G., Beyer, K., Penna, A., 2017. Material characterization for the shaking-table test of the scaled prototype of a stone masonry building aggregate. *17th ANIDIS Conference*, September 17-21, Pistoia, Italy.

Guerrini, G., Senaldi, I., Graziotti, F., Magenes, G., Beyer, K., Penna, A., 2019. Shake-table test of a strengthened stone masonry building aggregate with flexible diaphragms. *International Journal of Architectural Heritage*, in press.

Kallioras, S., Graziotti, F., Penna, A., 2019. Numerical assessment of the dynamic response of a URM terraced house exposed to induced seismicity. *Bulletin of Earthquake Engineering*, **17**(3), 1521-1552.

Lagomarsino, S., Penna, A., Galasco, A., Cattari, S., 2013. TREMURI program: an equivalent frame model for the nonlinear seismic analysis of masonry buildings. *Engineering Structures*, **56**, 1787-1799.

Penna, A., Lagomarsino, S., Galasco A., 2014. A nonlinear macroelement model for the seismic analysis of masonry buildings. *Earthquake Engineering & Structural Dynamics*, **43**(2), 159-179.

Penna, A., Senaldi, I., Galasco, A., Magenes, G., 2016. Numerical simulation of shaking table tests on full-scale stone masonry buildings. *International Journal of Architectural Heritage*, **10**(2-3), 146-163.

Senaldi, I., Guerrini, G., Comini, P., Graziotti, F., Magenes, G., Beyer, K., Penna, A., 2019. Experimental seismic response of a half-scale stone masonry building aggregate. *Bulletin of Earthquake Engineering*, in press.

Senaldi, I., Guerrini, G., Scherini, S., Morganti, S., Magenes, G., Beyer, K., Penna, A., 2018. Natural stone masonry characterization for the shaking-table test of a scaled building specimen. *10th International Masonry Conference*, July 9-11, Milan, Italy.

Wenk, T. Fäh, D., 2012 Seismic Microzonation of the Basel Area. *15th World Conference on Earthquake Engineering*, September 24-28, Lisbon, Portugal.